REVUE ROUMAINE DE GÉOLOGIE

ROMANIAN JOURNAL OF GEOLOGY

Tomes/volumes 64–65 **2020–2021**

SOMMAIRE / CONTENTS

Études et communications / Papers

FLUID AND MELT INCLUSIONS STUDY RELATED TO THE MAGMATIC-HYDROTHERMAL APATITE-ANHYDRITE ASSOCIATION FROM VOIA PORPHYRY CU-AU-(MO) PROSPECT (METALIFERI MOUNTAINS, ROMANIA)

IOAN PINTEA[1*], ION BERBELEAC[2], SORIN SILVIU UDUBAȘA[3], LUISA ELENA IATAN[2], MARIA-LIDIA NUȚU-DRAGOMIR[2]

[1]Geological Institute of Romania, Bucharest, Cluj-Napoca branch, Romania
[2]Institute of Geodynamics of Romanian Academy, Bucharest, Romania
[3]University of Bucharest, Faculty of Geology and Geophysics, Bucharest, Romania
* Corresponding author: ipinteaflincs@yahoo.com

Abstract. The study presents introductory data, based upon fluid and melt inclusion petrography, microthermometry and preliminary Raman spectra from a specific veinlet association formed by K-feldspar – biotite – quartz – anhydrite – apatite – albite – (Fe-Ti) oxides – sulfides, sampled in two sites from two drill holes from the central part of the complex porphyry – Cu-Au (Mo), HS- and LS- epithermal mineralizations from Voia prospect in the Metaliferi Mountains (Romania). Glassy and silicate melt inclusion showed Th between 800–950°C, sometimes more than 1000°C. Brine inclusion microthermometry showed Tm halite between 323°–594°C and Ws = 40–72 wt% NaCl eq., respectively. Minimum trapping temperature ranged between 436° and 973°C by vapor homogenization and between 429° and 594°C by halite homogenization, suggesting a continuous brine (salt melt) separation from silicate melt by immiscibility and successive boiling episodes, vapor-rich counterparts being always present. Calculated pressure suggested a mediated depth of brine inclusion entrapment around 3 km.

Keywords: fluid and melt inclusions, anhydrite, apatite, quartz, microthermometry, Voia porphyry Cu-Au (Mo).

Résumé. Cette étude présente des dates introductives obtenus par la pétrographie, la microthermométrie et par les spectres Raman préliminaires sur une association minéralogique spécifique de feldspath-K – biotite – quartz – anhydrite – apatite – albite – oxydes de Fe-Ti – sulfures, mesurées sur des échantillons de deux forages situées dans la partie centrale du complexe des minéralisations porphyriques de Cu-Au(Mo) et minéralisations épithermales de type HS et LS du projet minière de Voia, dans les Montaignes Métallifères en Roumanie. Les inclusions vitreuses et magmatiques montrent une Th entre 800°–950°C, d'ailleurs presque de 1000°C. La microthermométrie des inclusions hydrosalines montre la dissolution de l'halite entre 323°–595°C et une salinité de 40–72 wt% NaCl eq. La temperature minimale de piégeage mesurée varie entre 436° et 973°C, d'après l'homogénéisation de phase vapeur et entre 429°C et 594°C, d'après l'homogénéisation de l'halite, en suggérant la continuité de séparation d'une fondue hydrosaline de la liquide siliceux/silicaté par immiscibilité et ébullition successives, les vapeurs équivalents étaient toujours présents. La pression calculée suggère le piégeage des inclusions hydrosalines à une profondeur d'environ de 3 km.

Mots-clés: inclusions fluides, inclusions magmatiques, anhydrite, apatite, la microthermométrie, minéralisation porphyre Cu-Au(Mo) de Voia, Romania.

1. INTRODUCTION

The Voia porphyry Cu-Au(Mo) prospect is situated in the central-southern part of the Golden Quadrilateral in Metaliferi Mountains of the South Apuseni Mountains unit in western Romania. The area is situated at 4 km N from Hondol and 7 km NW from Săcărâmb old mining centers (Fig. 1). The interested exploratory prospect was documented on a surface area of about 10 km^2 based upon intense exploration works in the last decades (Berbeleac *et al.*, 1985, 2014, 2015, and references therein; Fig. 2).

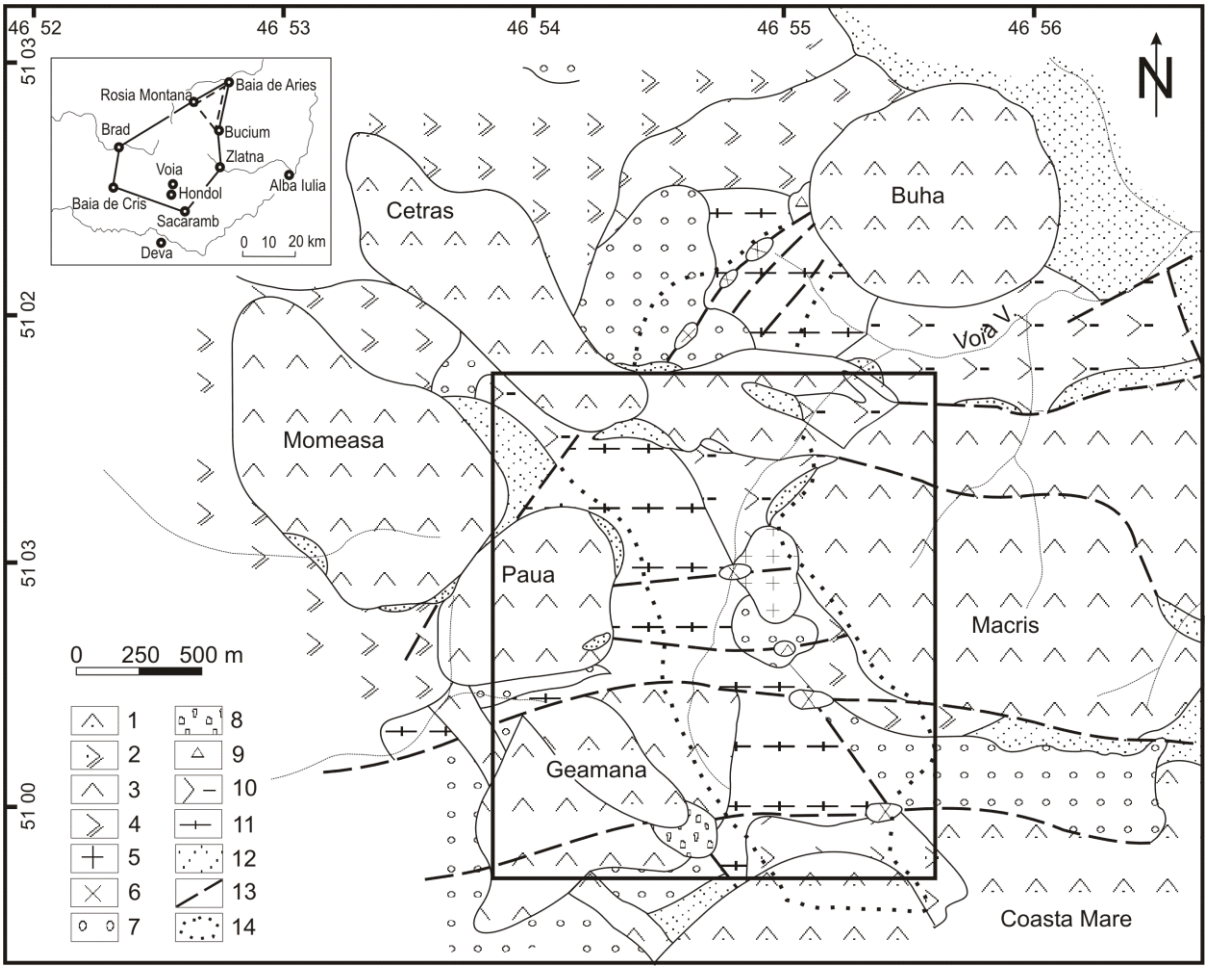

Fig. 1. Geological map of the Voia region (modified after Berbeleac *et al.*, 2015). Legend: 1) Hb, Bi, Qtz ± Px andesite (Cetraș type); 2) Lava flows of Hb, Bi, Qtz ± Px andesite (Cetraș type); 3) Hb, Qtz ± Bi, Px andesite (Momeasa type); 4) Lava flows of Hb, Qtz ± Bi, Px andesite (Momeasa type); 5) Qtz, Hb ± Bi andesite (surface subvolcanic body); 6) Dyke of Hb, Qtz andesite; 7) Badenian pyroclastic andesite; 8) Gold vuggy breccia; 9) Py hydrothermal breccia; 10) Intercalation of hybrid rocks with Badenian pyroclastic andesite; 11) Badenian-Sarmatian volcano-sedimentary rocks; 12) Upper Cretaceous-Paleogene Fața Băii Formation;13) Fault; 14) Contour of intense argillic alteration. Abbreviations: Hb= hornblende, Bi= biotite, Qtz= quartz, Px= pyroxene, Py= pyrite.

There are several polystadial mineralization phases, including an iron-rich porphyry Cu-Au (Mo), and HS (high-sulfidation) and LS (low-sulfidation) epithermal stages as veins and brecciated stockworks, overprinting successive andesite-microdiorite intrusions (Fig. 2). Various pyrite-chalcopyrite Ca-Mg skarn features were mentioned between quartz andesite-quartz microdiorite and limestone country rocks (Berbeleac, 1998).

A detailed exploratory program was based upon 18 diamond drilling boreholes (EDD), totalizing about 15,000 m. A deep structural image was defined by field mapping, geophysical investigations (Andrei, Ionescu, 1973), laboratory studies, and 29 MTS (magnetotelluric sounding) data interpretation down to 5,000 m deep (Berbeleac *et al.*, 2012, and Fig. 3).

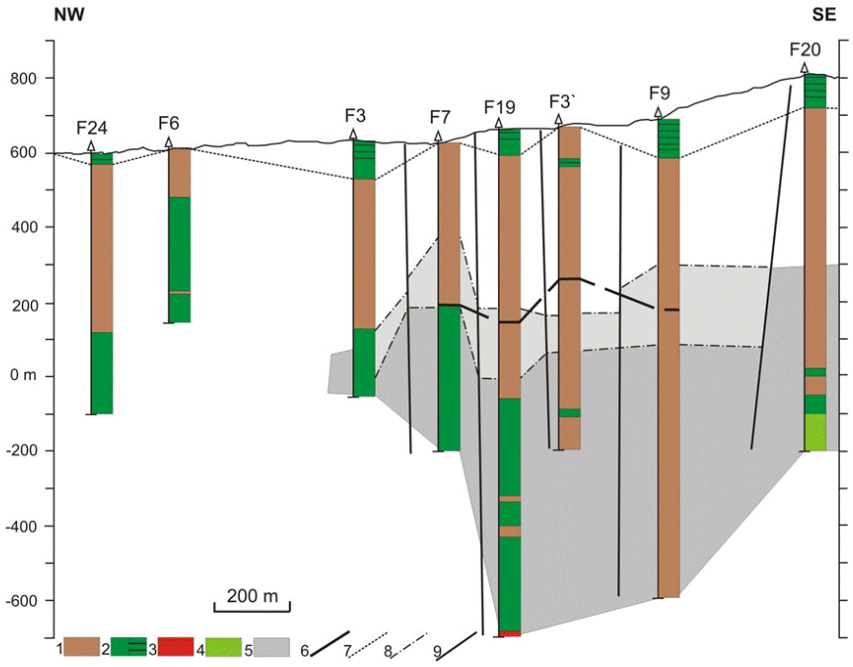

Fig. 2. Geological cross-section through the Voia subvolcanic body (after Berbeleac *et al.*, 2015). Legend: 1) Badenian-Sarmatian quartz andesite and microdiorite (partial mineralized sedimentary rocks); 2) Badenian-Sarmatian a. Sedimentary rocks, and b. Volcano-sedimentary rocks; 3) Upper Jurassic ophiolites; 4) skarned Upper Jurassic-Lower Cretaceous limestones; 5) Sarmatian porphyry mineralization in predominantly microdiorite rocks; 6) Approximated lower limit of intense argillic alteration; 7) Upper limit of Sarmatian volcano-sedimentary formation; 8) Sarmatian porphyry intrusions of quartz andesite-microdiorite as sheeted dykes, with mineralization; 9. Fault.

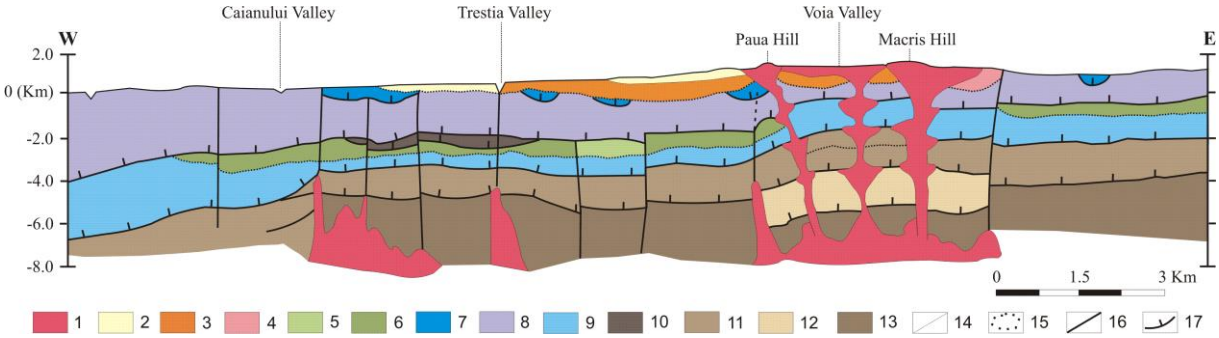

Fig. 3. Geo-tectonic section across South Apuseni Mountains (modified after Ştefănescu, 1986). Legend: 1) Miocene volcanic rocks; 2) Late Miocene sedimentary deposits; 3) Upper Cretaceous-Lower Miocene (Faţa Băii Formation) sedimentary and volcano-sedimentary continental deposits; 4) Upper Cretaceous-Paleogene (Faţa Băii Formation) volcano-sedimentary deposits; 5) Barremian-Aptian sedimentary deposits; 6) Barremian sediments; 7) Late Jurassic-Early Cretaceous limestone; 8) Middle Jurassic ophiolites – Late Jurassic calc-alkaline island arc volcanic rocks; 9) Late Jurassic-Early Cretaceous sediments ± ophiolites-nappe; 10) Paleozoic schist; 11) Muncel-Baia de Arieş nappe (?); 12) Curechi-Stănija Unit (?); 13) Biharia Unit (?); 14) boundary; 15) unconformity; 16) fault; 17) nappe.

2. MATERIAL AND METHODS

A batch of samples selected from an old drilling program (Berbeleac *et al.*, 1985) designed inside the Voia exploration district was investigated by fluid and melt inclusion study. One hundred thin sections, thirteen double-polished sections were prepared from different EDD and different depths, and used for petrographic observations. Two of them (from drills no. 19 and 9 – see Fig. 1 for location) were selected for microthermometry and Raman spectroscopy.

2.1. VEINLET MICROTEXTURE FEATURES

There are several types of veinlets separated from the studied drill holes samples, and prepared for fluid inclusion analysis. They are the followings:

- **Type A** veins (Fig. 4) containing K-feldspar + biotite + quartz + anhydrite I + apatite + magnetite + hematite + ilmenorutile + sulfides (pyrrhotite + pyrite I + chalcopyrite);
- **Type B_1** (Fig. 5**)** composed by quartz – anhydrite I (± apatite) + rutile (ilmenorutile) + pyrite I + chalcopyrite + hematite;
- **Type B_2** formed by quartz - anhydrite I + anhydrite II (± sulfide and/or sulfosalts + magnetite + hematite ± albite);
- **Type C** composed mainly by pyrite II + quartz ± anhydrite III + Na and K alunites (Berbeleac, 1970) + gypsum ± albite.

As a general feature, all of them show a strong, cohesive grained microtexture, especially by quartz and anhydrite formed by "in situ" recrystallization with the opaque grains stocked within grain intersection (mostly at $\theta = 120°$, dihedral wetting angle) and fluid (vapor-rich) wetting locally the edges of the subgrains, when they are present. Dihedral angle of $\theta > 60°$ is characteristic for type B_1 and B_2, and C is obviously marked by $\theta < 60°$ between quartz grains favoring fluid percolation, which developed finally to cvasi-parallel fissuration microtexture due to the intense fluid flushing substages. As it is suggested by the fluid and melt inclusions typology from quartz, anhydrite, and apatite, the type A veins were recrystallized from a complex hydrous silicate-sulfate melt, rich in chlorides and sulfur dominated gases (probably SO_2 and H_2S), often showing an equilibrium – microtexture (eutectic -?- Ducea *et al.*, 1999), formed mainly by quartz and anhydrite ± albite, type B mostly by a mixture of hydrosilicate-sulfate-chloride fluids (heavy fluid -?- e.g. Kotelnikov, Kotelnikova, 2010), where obviously anhydrite is mostly restitic (breakdown remains) and the new anhydrite (II) makes a specific association with specularitic hematite and rutile (ilmenorutile). Type C is representative for the late hydrothermal event of the porphyry stage (vapor expansion stage-?) with delicate pyrite – quartz (± sulfosalts) veinlets cross-cutting the former veinlets microtexture and frequently are formed inside the central part of the type A (rarely) and B (frequently) inducing a characteristic alteration halo around them. Type A has no alteration halos, and quartz grains (quartz eyes) show very intensely internal zonation (see Figs. 4 and 5).

There are two types of quartz eyes (Fig. 4) represented by isolated or agglutinated grains, rounded, with resorption, which probably are the primary quartz phenocrysts of the felsic component (former dacite or rhyolite before magma mixing or mingling) and the second type of quartz eye fragmented and randomly distributed inside of the rock groundmass, and frequently remobilized within the veinlets assemblages. Most probably are restitic fragments from an earlier porphyry stage being similar in composition and fluid and melt inclusions content as the type A vein does (Fig. 5). Perhaps the CL/SEM/EDS methods will be very useful in deciphering such a complex quartz internal microtextural features (Penniston-Dorland, 2001; Rusk, Reed, 2002; Vasyukova, 2011; a.m.o.).

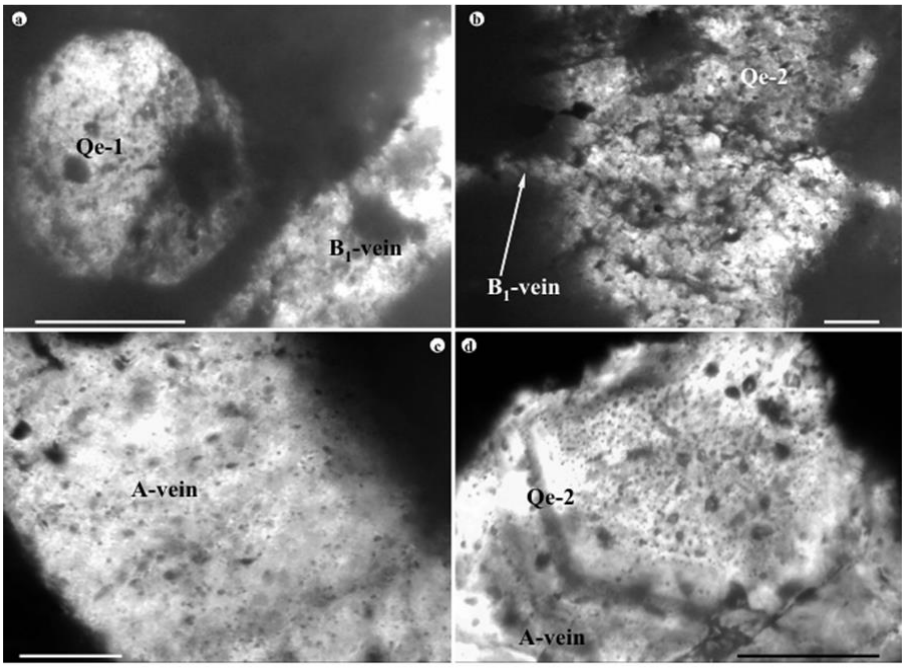

Fig. 4. Typical quartz host of the fluid and melt inclusions from Voia cutting samples. **a**. Qe-1 – quartz eye with embayments nearby a B_1 veinlet mainly with quartz grain and anhydrite + opaque; **b**. B_1 veinlet cross-cutting a relic of former quartz A vein; **c**. type-A veinlet with quartz and anhydrite without alteration hallo (near the magmatic stage); **d**. zoned quartz grain microcrystal, (Qe-2) from A-type veinlet, Scale bar: 1 mm.

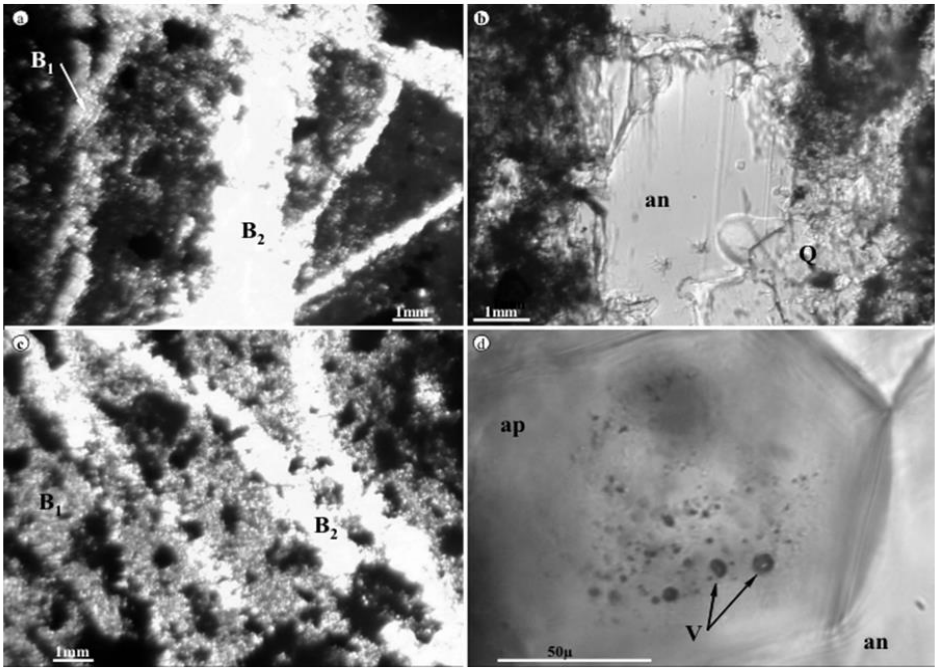

Fig. 5. Cross-cutting relations between B_1 and B_2 veinlets in microdiorite from Voia (**a, b**, and **c**); **d.-** Vapor-rich inclusion in apatite from anhydrite (second generation, probably crystallized from the magmatic vapor phase, suggested by the presence of the rhombohedral pyramids and triangular etches in anhydrite – e.g. Jakubowski *et al.*, 2002). Ap – apatite, an – anhydrite, V – vapor, Q – quartz.

2.2. FLUID AND MELT INCLUSION TYPES

Based upon the nature and number of the phases present at room-temperature condition, there are several distinctive types of fluid and melt inclusions trapped in quartz, anhydrite and apatite, representative for several magmatic-hydrothermal stages (mainly two with multiple pulses) distributed as primary, pseudo-secondary, and secondary assemblages.

I. Glass inclusions, which are frequently monophasic (often could be confused with solid microcrystal inclusion) composed of a vitreous shiny-luster body of glass and/or containing one or more vapor bubble, solid triangular microphases (chalcopyrite or nantokite – Pintea, 2009; Fig. 5), opaque ilmeno-rutile etc. showing bi- and multiphasic assemblages. The inclusions are randomly distributed or agglutinated, frequently showing a large size distribution from several microns to hundreds of micrometers. Frequently are rounded even perfect spherical objects suggesting their initial molten state. Often contain immiscible salty phases (chloride and/or sulphate) segregated as tiny rounded globules, now formed by solid, liquid and vapor phases. Mentioned also in others porphyry copper mineralizations from Metaliferi Mountains (e.g. Pintea, 1993a, 1996, 2009, 2014a, 2016) they are still problematic kind of silicate or complex silicate-sulfate melt among silicate melt type inclusion in porphyry copper (e.g. Eastoe, 1978; Pintea, 1993a, 2009).

II. Silicate melt inclusions, recrystallized after trapping, containing vapor bubble (10–30 vol %) and solid silicate-, sulfate-, chloride-, oxide-, and sulfide phases, representative for homogeneous or heterogeneous melt droplets trapped as inclusions mainly in quartz grains and rarely in anhydrite and apatite. They are primary, isolated or randomly distributed but could also be secondary and pseudosecondary trails assemblages decorating successive microfissure planes.

At room temperature conditions are frequently opaque, but during heating, under the microscope, the trapped phases become visible as temperature increase (Student, Bodnar, 2004).

III. Brine inclusions. Representative for multiphase inclusions formed by multiple solid daughter minerals as transparent phases (halite, anhydrite, salt-hydrates, feldspar, mica, etc.) besides opaque oxides (hematite, magnetite, rutile, ilmenorutile) and sulfides (chalcopyrite, pyrite, pyrrhotite, and sulfosalts) together with vapor and liquid phases. Three subtypes are envisaged:

IIIa. Homogeneous, with vapor bubble around 40 vol %, halite, anhydrite, hematite, sulfide, homogenizing by ultimate vapor bubble disappearance;

IIIb. Heterogeneous, with almost the same composition but the vapor bubble occupies less than 20 vol % from the cavities, homogenizing by ultimate halite dissolution frequently in the presence of anhydrite, alunites-?, hematite, and others;

IIIc. Vapor-rich, formed by a dominant vapor bubble (around 80 vol %) and halite, anhydrite, and silicatic daughter phases typical for fumaroles (e.g. Pintea, 2014b).

Generally, these inclusions show immiscibility as exsolved phases from the silicate melt (salt globules) or separated by successive boiling episodes associated with vapor-rich inclusion counterparts. It could be primary, when they decorated growth mineral zones and randomly distributed in a cluster or isolated cavities. Pseudosecondary and secondary inclusions decorating multiple microfissure planes are specifically for each grain but rarely cross-cutting two or more grains in the same direction (characteristic planes for the late stages of fluid evolution). Obviously, they are very small, frequently below 1–5 microns, but there are also cavities between 10–15 microns that could be used for microthermometry purposes (Fig. 6). Sometimes these inclusions show cloudy distribution suggesting a spraying process inside the former silicate matrix, now trapped in recrystallized quartz. All together are representative for high salinity and high-temperature brine, responsible for transport and deposition of the ore element in potassic and sericitic (anhydrite) zones via fluid phase separation by

boiling (immiscibility) vapor contraction, condensation and expansion (e.g. Heinrich *et al.*, 2004; Henley, Berger, 2011). In the earlier phases (purely magmatic) they were separated directly from the melt as the crystallization of the magma chamber proceed. Moreover, the vapor-rich fluid phase (V) would be understood as an unconventional fluid type (e.g. fl – bubble in Fig. 7), i.e. hydrosilicate vapor – "melt" inclusion as it was emphasized recently in the porphyry copper system by Wilkinson *et al.* (2015).

IV Aqueous biphasic fluid inclusions with two subtypes:

IVa (L+V), dominated by a low salinity liquid (< 23. 18 wt % NaCl eq.) containing a vapor bubble of less than 50% in volume;

IVb (V+L), where the vapor phase occupies around 80–90 % of the cavity volume. They are frequently counterparts of contemporaneous silicate, brine or aqueous inclusions, being composed mainly of a less dense aqueous vapor phase. Usually, they are primary, in the late stage of quartz and anhydrite II (or III), frequently are distributed as trails (pseudosecondary and secondary) in the quartz veins overprinting the primary magmatic-hydrothermal stages. Frequently, mainly in the quartz eye grains, all types of above-described fluid and melt inclusion could be present as separate trails in various cross-cutting time relations. That is the case for multistage fluid evolution when the former fluid and melt inclusions are of multiple types and generations.

V. Monophasic fluid inclusion, entirely filled-up by a liquid aqueous phase or a less dense vapor phase. Many of them could be representative for a supercritical pure H_2O fluid forming characteristic cluster association, frequently bearing sulfide (e.g. triangular chalcopyrite) or submicronic salt or silica particle, as always were described in the Miocene porphyry copper deposits from Metaliferi Mountains (Pintea, 2010, 2016).

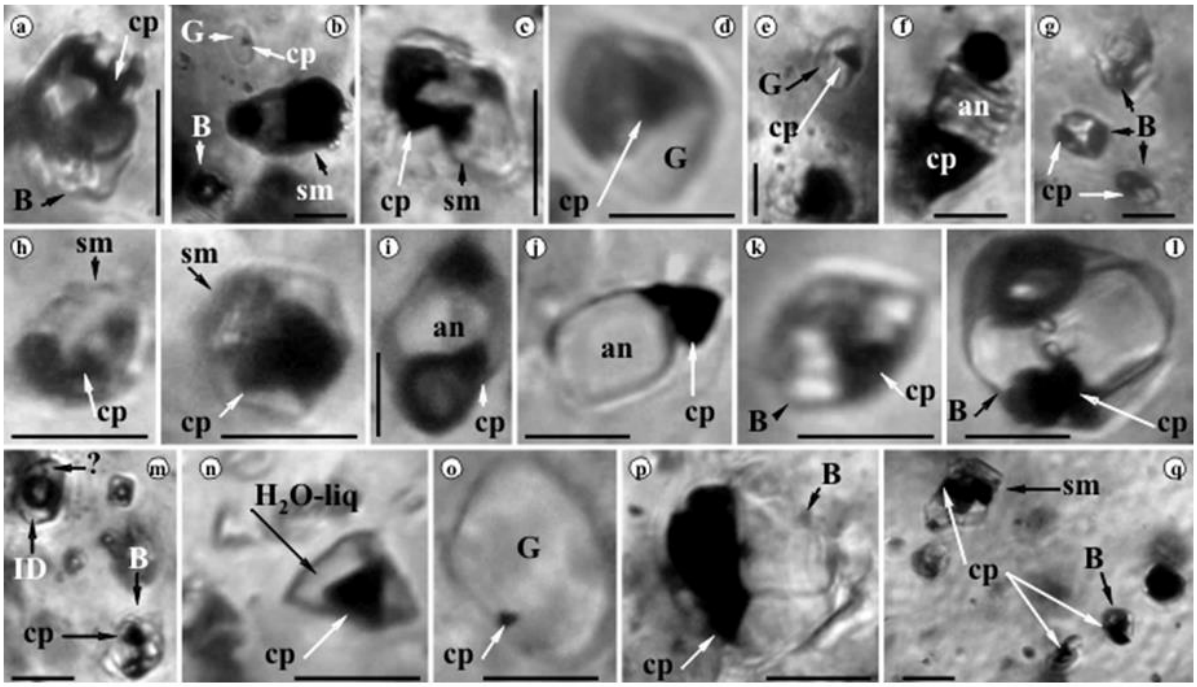

Fig. 6. Opaque triangular platelets of chalcopyrite (or nantokite) in various types of fluid and melt inclusions from the Voia porphyry copper deposit. B – brine inclusions, G – glass, cp- chalcopyrite (or nantokite), sm – silicate melt inclusions, an – anhydrite, ID – intermediate (L+V) density fluid inclusion. Scale bar: 10 μm.

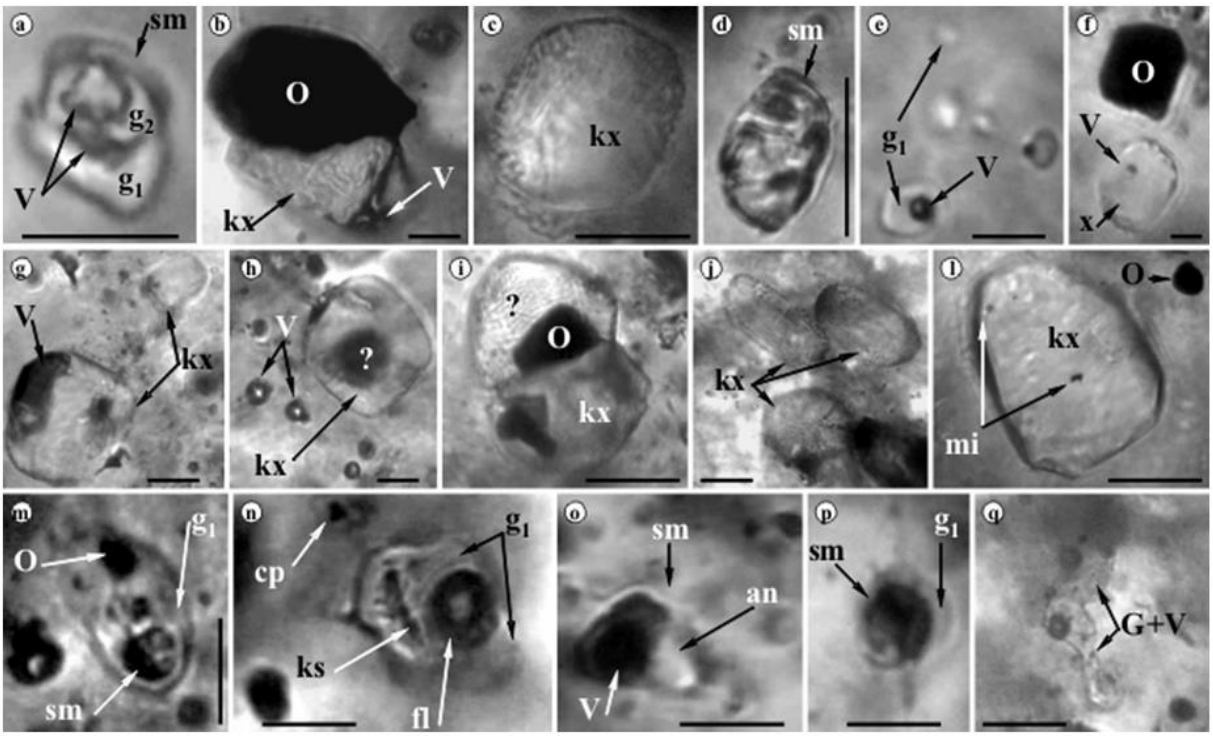

Fig. 7. Quenching feature in silicate melt and glassy inclusions after heated up to 950–1050°C, during the homogenization experiments under the microscope. **a.** former crystallized complex silicate melt inclusion segregated two immiscible phases at high temperature quenched in two glass types + vapor + a small unknown microcrystal; **b., c., f., g., h., i., j., l.,** – superficial melted film around glass inclusions, vapor and microsolid phases appeared at high temperature up to 800°C, suggesting that the solid body of inclusion was partially remelted and released melt and volatile phases; **d.** remelted glass inclusions and recrystallized after quenching, separated several solid microcrystal and vapor bubbles; **c**. tiny silicate melt inclusions initially completely devitrified were almost homogenized at high temperature, showing now a vapor bubble inside the silicate glass phase (similar to the sample VIB 9 in Table 1); **m., p.** immiscibility between silicate melt (now glass) and salt melt (salt crystal + vapor + liquid); **o.** two immiscible phases were in equilibrium up to 993°C between a silicate melt and salt liquid (chloride or sulfate), now represented as initially phase state by the recrystallized solid phases in the glass matrix; **n., q.** vapor bubbles and solid microparticles in glass matrix quenched from around 1000°C to room temperature. Notation: g_1, g_2 – silicate glass inclusions (unknown composition), O – opaque (mainly as Fe-Ti oxide globules,), kx – unknown solid microcrystal, x – microcrystal or glass inclusion, sm – salt melt, cp – chalcopyrite, fl – fluid phases, an – anhydrite, G – silicate glass, V – vapor, ? – vapor or opaque. Scale bar: 10μm.

VI. Microsolid inclusions described as follows:

VIa. Opaque granular globule, euhedral or mainly rectangular or polyhedral composed of oxide and sulfide microphases could also be restitic phases (mafic alteration product), especially formed by agglutinated grains of anhydrite, Fe-Ti oxide and apatite. Very often, they are clustering abundantly in specific association of globular inclusions in quartz and anhydrite. Probably formed by Fe-Ti oxide microminerals (rutile, magnetite, hematite, ilmenorutile) and globular sulfide (pyrite, pyrrhotite or chalcopyrite) in primary and secondary (or pseudosecondary) assemblages. Various in size, from 10–25 microns to 100 microns or more. Frequently they were trapped accidentally in silicate, brine and aqueous fluid inclusions, probably being the main cause of inclusion formation. There are at least 2–3 generations of globular inclusions inside the quartz veinlet formed during the alteration-mineralization processes. They are vector minerals in porphyry copper exploration and hydrometallurgical processes for the main elements and by-product recovery in the modern mining industry (e.g. Williams, Cesbron, 1977; Meinhold, 2010).

VIb. Transparent micromineral inclusions, formed by euhedral or rectangular grains of anhydrite, apatite and zircon. Frequently are relict of former minerals showing rounded, elongate forms distributed in aggregated clusters or parallel to the growth zones or trails in cicatrized microfissure planes. These restitic phases are good indicators of sulfur degassing of magma during the final stages of crystallization and porphyry copper formation (e.g. Streck, Dilles, 1998; Dilles *et al.*, 2015). In the mineralized porphyry copper system from Voia there are also 2–3 generations of apatite and anhydrite, formed in various magmatic-hydrothermal conditions as suggested by their fluid and melt inclusion assemblage content.

3. MICROTHERMOMETRY

An experimental evaluation study was made for silicate melt and brine inclusions from two samples selected from Drill hole no. 19 and no. 9 situated in the central part of the crystallized porphyry copper stock (Berbeleac *et al.*, 1985). All measurement was made in a "made in house" device operating at low magnification in the interval of 25° to 1100°C and 25° to 800°C for the high magnification lens (40×), calibrated with K-dichromate (398°C), α↔β transition in synthetic quartz (573°C), and pure gold (1064°C). The accuracy of phase change measurement ranged between ± 15°C. Calculated PTX data in Table 1 were based upon Sowat programs (Driesner, Heinrich, 2007).

3.1. GLASSY AND SILICATE MELT INCLUSION MICROTHERMOMETRY

Because of the small size of the inclusions, only a 40× lens was used, and the final temperature in the stage was situated around 850–900°C, rarely more because of protective technical reasons. Up to this higher temperature, final homogenization (minimum trapping temperature) was never achieved (except one value recorded at ≥1040°C for a tiny silicate melt inclusion noted in Table 1) due to several inconveniences such as heterogeneous trapping, anhydrite daughter microcrystals do not entirely melt in the silicate melt liquid, opaque minerals also remained partially melted, vapor bubble often disappeared before solid microphase dissolution (Fig. 7). As a preliminary estimation, we estimated that silicate melt inclusions and also glass inclusions were trapped at min. 800–950°C, most probably around 1040–1050°C based upon anhydrite coexistence temperature with trachyandesitic and rhyolitic silicate melt, over the temperature range of 1040–800°C (Carroll, Rutherford, 1987), temperature stability interval for the andesite host rock (e.g. Pintea, 2014b), and also in agreement with Burnham's genetic model for porphyry copper deposits applied to similar porphyry copper deposits in the area (Pintea, 2014a).

3.2. BRINE INCLUSION MICROTHERMOMETRY

The complex multiphasic brine inclusions showed two homogenization modes as noted in Table 1, i.e. one by halite dissolution first and then vapor bubble disappeared (e.g. Fig. 8) and secondly the reversal mode when vapor bubble disappear first and then halite. It is important to note that in both situations, after homogenization temperature, there are one or more solid phases still undissolved or even regrowing ones. The system used for PTX- data calculation is H_2O-NaCl available for such a large temperature interval by using the two versions of the Sowat PC program (Driesner, Heinrich, 2007).

Halite melting temperature, Tm in Table 1, shows quite a homogeneous temperature interval between ≥ 323°C and 594°C, such as in other Miocene porphyry copper deposits from Metaliferi Mountains (e.g. Pintea, 1996, 2014a), allowing to calculate salinity between 40 and 72 wt % NaCl eq. The trapping temperature (T) was recorded between 436 and 973°C by vapor bubble disappearance and between 429 and 594°C, by halite homogenization, suggesting a continuous brine (salt melt) separation (fractionation-?) from the silicate melt by immiscibility and successive boiling episodes (vapor counterparts are always present), and also silicate and/or glass inclusion mentioned above.

Table 1

Microthermometric data for silicate melt and brine inclusions from samples VIB4 (F19 m 805) and VIB9 (F9m1145) from Voia prospect district. Notations: Tm – halite melting temperature, Th(L-V) – homogenization temperature by vapor bubble disappearance, T – minimum trapping temperature, red number* – halite homogenization temperature, Ws – salinity, SPS – single-phase state, V – vapor, L – liquid, H – halite. Depth estimation data suggested by Audetat *et al.* (2004) in a similar porphyry copper deposit containing magmatic anhydrite and calcite as primary phases.

Sample	Tm °C	Th(L-V), °C	T, °C	P, bar	Ws, wt% NaCl eq.	X, Mole fraction of NaCl	Density, g/cmc	Depth, km	Phase state at Th
VIB4	505	683	683	768.24	60.6032	0.32	1.0369	1.9	**V+L**
	505	704	704	825.198	60.6032	0.32	1.0256	2.2	**V+L**
	505	760	760	999.541	60.6032	0.32	1.0032	2.8	**SPS**
	500	973	973	1856.34	69.9042	0.32	0.95865	5.4	**SPS**
	416	897	897	1783.13	48.9713	0.22	0.85038	5.1	**V+L**
	457	477	477	308.104	54.0844	0.3	1.1096	0.9	**L+H**
	500	442	500*	771.419	59.6582	0.32	1.2046	2.3	**L+H**
	500	921	921	1644.15	59.9042	0.32	0.96563	4.5	**SPS**
	436	361	436	970.402	51.2753	0.3	1.1718	2.5	**L+H**
	544	631	631	560.09	66.1548	0.325	1.1455	1.7	**L+V**
	323	891	891	1827.65	39.5465	0.2	0.74255	5.1	**SPS**
VIB 9	429	336	429*	1263.4	50.3724	0.23	1.1832	3.4	**SPS**
	-	1048	1048	–	–	–	–	–	**melt±V**
	588	495	588*	1612.04	71.0816	0.45	1.327	4.5	**L+H**
	514	622	622	597.638	61.8702	0.3	1.09532	1.7	**SPS**
	355	639	639	906.995	42.4196	0.18	0.84891	2.6	**V+L**
	521	413	521*	1448.38	62.0718	0.33	1.256	4.2	**SPS**
	594	505	594*	1606.35	71.9056	0.44	1.3333	4.5	**SPS**
	517	724	724	849.58	62.2948	0.33	1.0368	2	**V+L**
	531	781	781	986.056	64.2889	0.35	1.0401	2.5	**V+L**

The final homogenization temperature (Fig. 8) was recorded, generally when the vapor bubble disappeared during the heating procedure in the stage (rarely by halite homogenization). Despite the fact that almost all bubbles dissolved at the temperature mentioned in Table 1 (T values), the calculated PTX properties by Sowat program (Driesner, Heinrich, 2007) show some variability around the phase state of the enclosed fluid/melt at the homogenization temperature. This could be related firstly to the fact that always the ideal H_2O-NaCl system is contaminated by other components in the solution like sulfate, silicate, and other chloride compounds (such as $FeCl_2$, $CaCl_2$ $MgCl_2$ etc.). Moreover, it is suspected that during heating-quenching cycles based upon direct observation, the main saline brine (i.e. NaCl) seems to interact with the sulfate (perhaps Na_2SO_4, Ca_2SO_4) to form some intermediate solid compound as it was predicted from recent experimental work by Newton, Manning (2005).

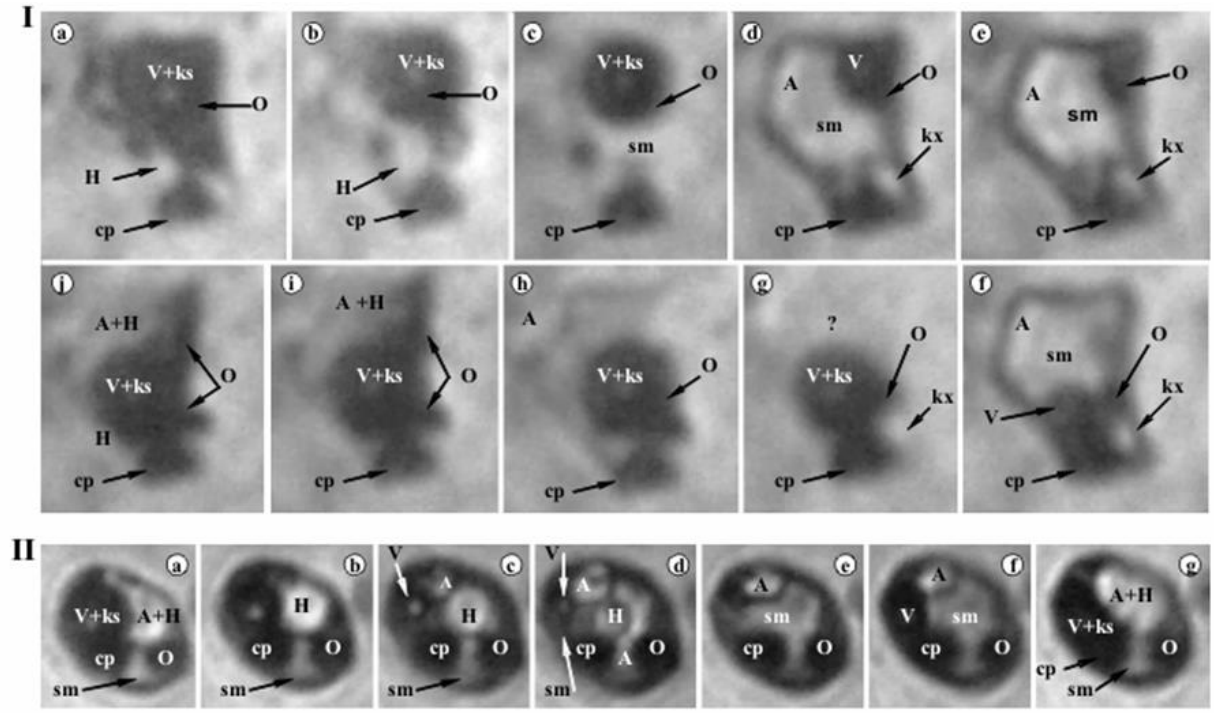

Fig. 8. Two serial microphotographs examples of the microthermometry experiments in the sample VIB9 (I) and VIB 4 (II) from Voia porphyry copper deposit, both homogenizing by vapor bubble disappearance. I-**a.**25°C, **b.**174°C, **c.**259°C, **d.**465°C, **e.**573°C, **f.**345°C, **g.**254°C, **h.**175°C, **i.**146°C, **j.**131°C; Tm=355°C, Th=639°C, W=42 wt% NaCl eq, d= 0.8 g/cmc; P= 0.9 kbar (aprox. 2.7 km)- present sample location: 1145 m depth); **II-a.**96°C, **b.**274°C, **c.**366°C, **d.**399°C, **e.**461°C, **f.**481°C, **g.**25°C; Tmh=457°C; Th= 477°C, W=54 wt% NaCl eq., d =1.1 g/cmc, P= 0.3 kbar (aprox. 0.9 km) – present sample location: 805m depth). V – vapor, ks – unknown daughter phase, H – halite, O – opaque, A – anhydrite, cp – chalcopyrite, sm – salt melt, ? – unknown phase. Both inclusions have around 10 μm in length.

The second observation is concerned about initial trapping fluid, which in this situation (i.e. Voia fluids) seems to suggest generally heterogeneous trapping where two or more liquids, gas and solid particles were trapped together in the cavities. As a general petrographic observation, anhydrite seems to be distributed pervasively in the veinlet system of the mineralized stock at Voia (Berbeleac *et al.*, 1985), and frequently seems to be the main cause of fluid and melt inclusions formation by adhering the solid microparticles to the surface of the growing host mineral, especially quartz. As a consequence, we consider that the measured temperature values are the real formation temperature between 429° and 1048°C, of the fluid and melt inclusions characterizing the main magmatic-hydrothermal regime from Voia porphyry copper deposit (the sample studied are from two central drill holes situated at 1145 and 805 m depth). Calculated pressure values suggested a mediated depth of brine inclusion formation around 3 km, which is in good agreement with some other porphyry copper formation depth condition about 1–4 km in similar volcanic environments (e.g. underlying magma reservoir at El Teniente porphyry copper deposit, for example, was situated around 4 km – Rabbia *et al.*, 2009).

3.3. PRELIMINARY RAMAN SPECTROSCOPY

Vibrational Raman spectra of brine and solid inclusions (transparent and opaque) from Voia quartz and anhydrite hosts (Table 2, Fig. 9a–d) were performed at the Geological Institute of Romania, assisted by res. assist. Oana C. Barbu on a Raman Renishaw spectrometer, equipped with a Leica DM 2700M and 50X objective lens. Excitation was provided by two laser types with 532 nm with

resolution of 1,200 l/mm to 1800l/mm and 785 nm with a resolution of 1200 l/mm, respectively. Laser time exposure ranged between 5 to 15 sec and counting time from 1 to 55.

Table 2

Main Raman vibration (cm^{-1}) of selected solid (mainly glass and opaques) and brine inclusions (polyphasic) from quartz and anhydrite of two samples from Voia porphyry copper prospect

No.	Sample no/Laser green wavelength	Host/Inclusion type	Raman shifts, cm^{-1}
1	VIB9R-2/785nm	Quartz host only	127, 206, 464, 590
2	VIB9R-4b/785nm	Quartz/solid inclusion (microcrystal or glass)	1211, 1316, 1396, 1762
3	VIB9R-6/785nm	Quartz/brine inclusion	1211, 1316, 1396, 1762
4	10VIB4-R-1/532nm	Anhydrite/Glass inclusion	121, 475, 497, 607, 626, 1016, 1456, 1519
5	12VIB4-R-3a/532nm	Anhydrite/Glass inclusion	121, 497, 607, 626, 1015
6	15VIB4-R-6/532nm	Anhydrite/Opaque inclusion	183, 287, 414, 1015, 1084, 1728

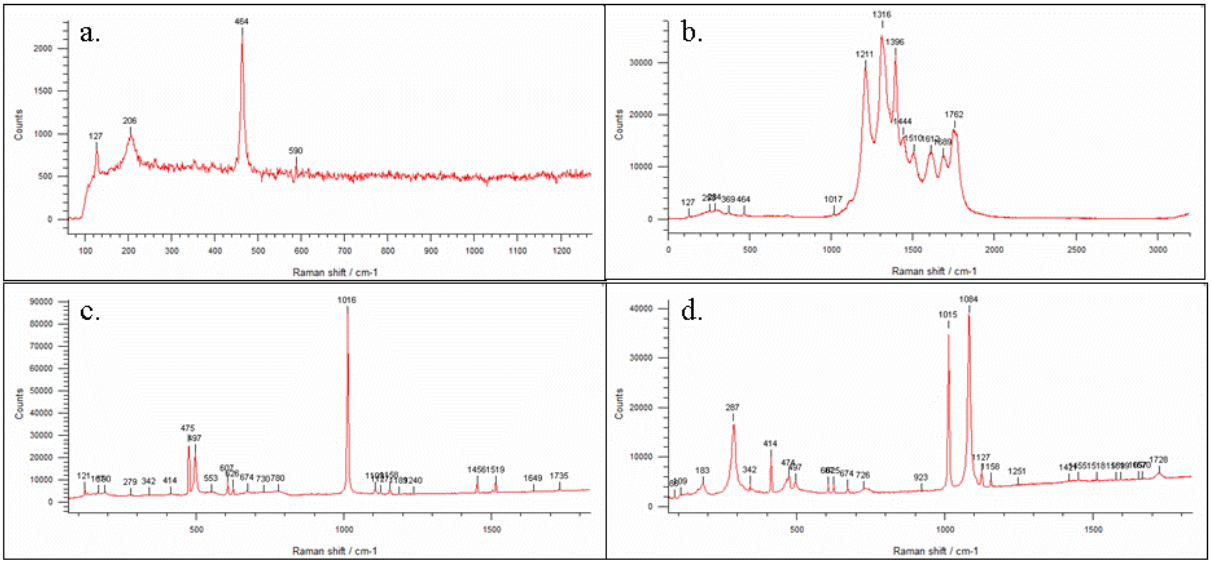

Fig. 9. Raman spectra in quartz and anhydrite from Voia prospect. **a.** quartz host, **b**. polyphasic inclusion (brine) in quartz, **c.** glass inclusion in anhydrite and **d.** opaque inclusion in anhydrite. See text for explanation and also Table 2.

In this analyzed session (Table 2) the quartz host is Raman active with the strongest characteristic peak at 464 cm^{-1} (Frezzotti *et al.*, 2012) and anhydrite with the highest peak at 1015 cm^{-1} (Burke, 1994). Concerning the silicate glass inclusions as a rounded object, colorless and/or brown, trapped in quartz and anhydrite, only the presence of SO_4^{2-} could be envisaged in glass at 1016 cm^{-1}, trapped together with an opaque grain supposed to be an Fe-Ti oxide grain by the stretching lower band in Table 2 (rows no 4, 5, 6). CO_2 band is specific between 1,316–1,396 cm^{-1} could be assigned in quartz samples (Table 2 rows no 1 and 2). Silica complexes between 475 cm^{-1} and 626 cm^{-1} peaks could be assigned too in the glass inclusions in anhydrite. Carbonates (CO_3^{2-}), especially calcite, have the highest vibration line at 1085 cm^{-1} and many weak vibration lines for $CaCO_3$ (156 and 284 cm^{-1}), $CaMg(CO_3)_2$ (176, 299 cm^{-1}), and $MgCO_3$ (212 and 329 cm^{-1}) very close to our data in Table 2 (rows 4, 5), (Frezzotti *et al.*, 2012).

4. THE ANHYDRITE ISSUE

The general observation that anhydrite presence encompassed the entire magmatic-hydrothermal domain at Voia (Berbeleac *et al.*, 1985) strongly suggests the oxidizing character of porphyry copper deposit formation conditions in the Metaliferi Mountains (Udubasa *et al.*, 2001). The presence of primary magmatic-hydrothermal anhydrite in the Voia andesitic and microdioritic rock as well in the central veinlet system of the mineralized porphyry stock revealed that the primary magmatic sulfur reservoir was recycled in the multistage evolution of this system (Fig. 10). There are three generations of anhydrite, apatite, and rutile minerals pervasively distributed in the studied representative samples, as preliminary petrography indicated. They also participated as solid microparticles in the brine and silicate melt inclusions from quartz, anhydrite, and apatite host minerals. We describe in this study based upon petrography and microthermometry, the presence of magmatic-hydrothermal anhydrite in the Voia multistage mineralized subvolcanic structure (these are preliminary data and they must be completed by other analytical methods!). The suspicious glassy, melt and opaque Fe-Ti oxide minerals embedded mainly in the late magmatic hydrothermal anhydrite suggested the presence of a volatile hydrous silicate – sulfate melt exolved to near magmatic temperature regime (Fig. 11). Fluid inclusions ranging from low to moderate temperature from porphyry copper ore deposits were described at Moldova Noua (Gheorghita, 1975) and in several Miocene porphyry copper systems from Metaliferi Mountains (Pintea, 1993b).

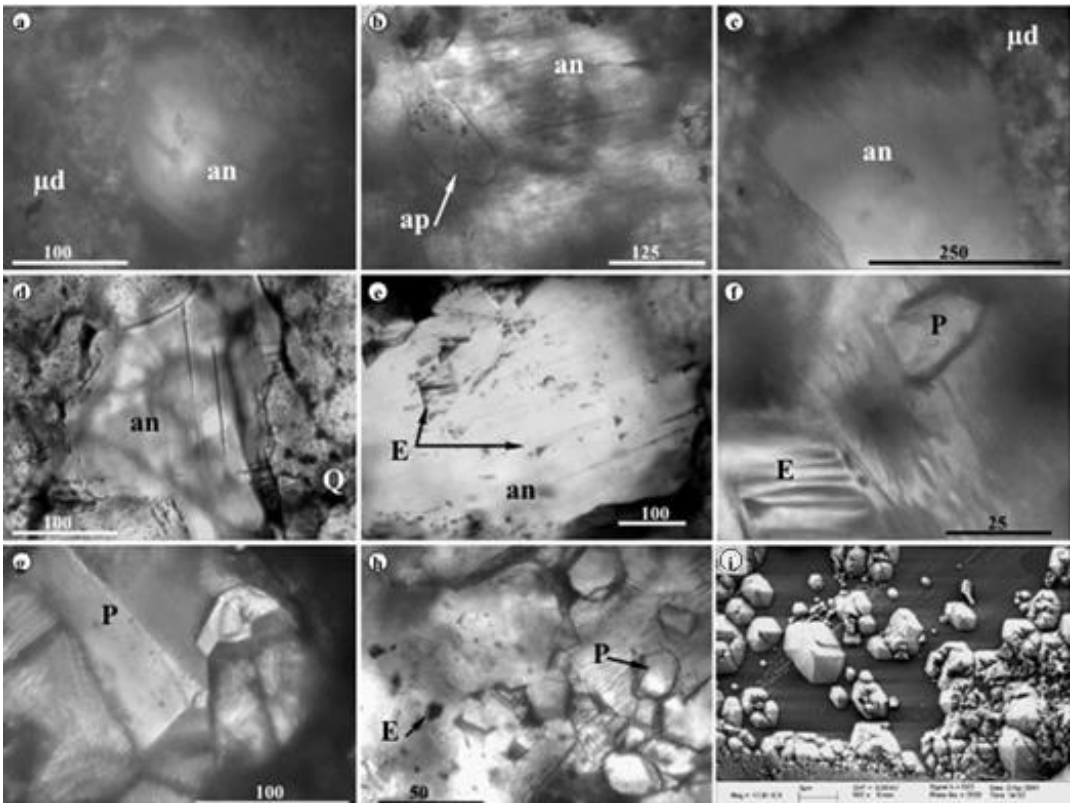

Fig. 10. Magmatic – hydrothermal anhydrite in the Voia porphyry-copper deposit. **a** to **c –** magmatic anhydrite phenocrysts (an) in microdiorite, including apatite (ap) with primary silicate melt inclusions in **b**; **d** – anhydrite relic in quartz grain in B – type veinlet; **e**, **f**, **g**, **h** – growing features in magmatic-hydrothermal anhydrite represented by etch pits (E) and pyramids (P); **i** SEM images displaying the pyramidal surface feature in Mt Pinatubo anhydrite (Jakubowski *et al.*, 2002) Scale bar in µm.

The presence of magmatic anhydrite in volcanic and subvolcanic rocks, even in granite pluton, was reported in many places worldwide (El Chichon – Luhr *et al.*, 1984; Pinatubo – Fournelle *et al.*, 1996, Pasteris *et al.*, 1996; Nevado del Ruiz – Fournelle, 1990; Santa Rita – Audetat *et al.*, 2004; Eagle Mountain – Parat *et al.*, 2002; The Cajon Pass Deep Scientific Drillhole – Barth, Dorais, 2002; El Teniente – Stern *et al.*, 2007; Yanacocha – Chambefort *et al.*, 2008).

Magmatic anhydrite crystals were found and described together with disseminated sulfide (i.e. pyrrhotite, pentlandite, and chalcopyrite trapped in anhydrite), olivine, and inclusions in augite (and vice versa) in the gabbros of the Kharaelakh intrusion from the Siberian Traps flood basalts (Li *et al.*, 2009). The occurrence of anhydrite in the porphyry copper system is a ubiquitous feature, mainly as a late hydrothermal alteration product (e.g Eastoe, 1978, 1982; Beane, Titley, 1981; Seedorff *et al.*, 2005; Johnson, Barton, 2005; and references therein).

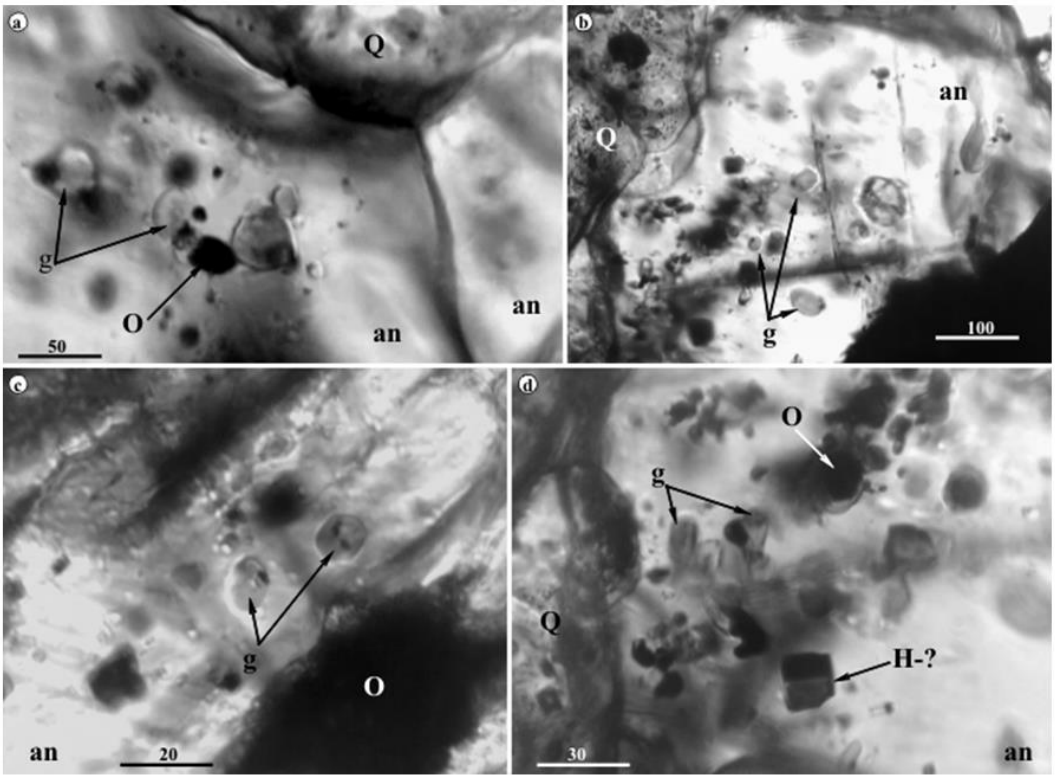

Fig. 11. Silicate glass inclusions (monophasic and biphasic) in magmatic-hydrothermal anhydrite from B – type veinlet with equilibrium recrystallization microtexture in the Voia porphyry copper deposit. **a.** triangular intersection (θ=120°) between quartz and anhydrite containing a cluster of silicate glass inclusion associated with opaque (Fe-Ti oxide); primary isolated (**c**) and clusters of silicate glass inclusions associated with opaque (**b**, **d**) and possible, solid halite inclusions (**d**); Notations: an – anhydrite, Q – quartz, g – silicate – sulfate glass (?), O – opaque (Fe-Ti oxides, mainly rutile), H – halite. Scale bar in μm.

The fluid inclusions contain obviously anhydrite daughter phases besides halite, sylvite and others in all porphyry copper deposits around the world, mainly Cretaceous and Neogene porphyry copper belts from North America, Andes, Circumpacific region, Asia, and Europe (John *et al.*, 2010). Anyhow, it remains problematic why so rarely was described as a magmatic-hydrothermal product in these common and productive ore deposits (sulfur dominated). For example, it was described as uncommon solid inclusions (glassy or micromineral inclusions) by Eastoe at Panguna (1978), in porphyry copper deposits from Romania (Pintea, 1993a, 2009), remaining an unsolved issue regarding

their presence in the characteristic stockwork environments. In Romania, as an alteration product, it was described in the majority of the alteration facies in the upper Cretaceous porphyry and skarn environments (e.g. Gheorghita, 1975) and in Miocene porphyry copper from Metaliferi Mountains also (Bostinescu, 1984, Berbeleac *et al.*, 1985; Milu *et al.*, 2004 and references therein). This study presents the first evidence of magmatic anhydrite based upon the presence of primary glass inclusions highlighted by optical microscopy and characteristic Raman spectra (Fig. 9 c,d and Fig. 11).

There are at least two possibilities to crystallize anhydrite in the magmatic evolution stage: one is magma saturation in sulfate in the late stage of crystallization as immiscible phase (e.g. droplets of carbonate melt were envisaged as second immiscibility in the complex silicate-salt inclusions at Vesuvius – e.g. Fulignati *et al*., 2001). The solubility of calcite and anhydrite in H_2O-NaCl solution at high temperature and pressure are quite similar (Newton, Manning, 2002 and 2005). For anhydrite, the experimental work of Caroll, Rutherford (1987) demonstrate that anhydrite may coexist with trachyandesite to rhyolite melt over the temperature range of 800° and 1040 °C, suggesting that this mineral was crystallized at magmatic condition in the Voia porphyry copper structure as the microthermometry has shown (Fig. 4 and Table 1).

So, it is quite possible that primary magmatic anhydrite phenocrysts envisaged in the microdiorite or andesitic host rocks at Voia by microscopy (preliminary!) should be indeed magmatic phenocrysts crystallized as a separate phase from an anhydrite saturated magma. During the high temperature autometasomatic thermic regime, anhydrite breakdowns easily forming the hydrosilicate – salt melt and generating the potassic alteration stage and finally preserved as complex silicate-, brine and vapor rich inclusions in quartz, anhydrite II, and apatite in the specific veinlet assemblages. Recrystallization from the volatile-rich silicate-sulfate melt is suggested by the common growing feature of anhydrite from experimental high P-T vapor phases (e.g. Jakubowski *et al.*, 2002), these being also emphasized in this study by optical microscopy in transmitted light (Fig. 6).

The second possibility of anhydrite formation was envisaged a long time ago by Holland, Malinin, 1979 (cited in Eastoe, 1982) by SO_2 rich vapor phases according to the reaction: $4SO_2 + 4H_2O = H_2S + 3H_2SO_4$. Recently, Henley *et al.* (2015), reiterated the importance of SO_2 deep magmatic supply during the basic recharging at the bottom of felsic shallow magma chambers. Gas chemisorption to the surface of feldspar could produce a rich anhydrite layer by the reaction $2CaAl_2Si_2O_8 + 3SO_{2(g)} \rightarrow 2CaSO_4 + 3Al_2SiO_5 + 3SiO_2 + H_2S_{(g)}$. The reaction between vapor and brine could also be a common mechanism to produce anhydrite and other sulfur components in the magmatic-to-hydrothermal evolution of the porphyry copper systems (Blundy *et al.*, 2015).

5. CONCLUSIONS

The main conclusions of this study are the followings:

1. The Tertiary porphyry (Fe)-Cu-Au(Mo) Voia prospect from Metaliferi Mountains (W-Romania) contains multiple apatite – anhydrite magmatic-hydrothermal associations;
2. The potassic sequence of K-feldspar – biotite – quartz – anhydrite – apatite – albite – (Fe-Ti) oxides ± sulfides contains various fluid and melt inclusions assemblages;
3. Glassy and silicate melt inclusions show Th between 800–950°C, sometimes more than 1000°C; Brine inclusion microthermometry shows Tm halite between 323°–594°C and Ws = 40–72 wt% NaCl eq., respectively. Minimum trapping temperature ranged between 436° and 973°C by vapor homogenization, and between 429° and 594°C by halite homogenization, suggesting a continuous brine (salt melt) separation from silicate melt by immiscibility and successive boiling episodes, vapor-rich counterparts being always present. Calculated pressure suggested a mediated depth of brine inclusion entrapment around 3km;

4. There are at least two generations of anhydrite – apatite association (or parageneses?) formed in the magmatic-hydrothermal stage at high P-T conditions, most of them deposited from a hydrous silicate – sulphate – chloride melt exsolved as vapor rich fluid from the silicate magma. Specifically, anhydrite and apatite contain silicate glass and vapor-rich inclusions assemblages, which, combined with characteristic microtexture features of the hosts, are indeed suggestive for their deposition from a vapor-dominated melt. Future elaborated work would be necessary to be done for deciphering the fluid-melt evolution in the Voia complex prospect.

Acknowledgements. We thank to research Assistant Oana C. Barbu from IGR-Microcosmos-laboratory for her precious assistance during Raman spectroscopy analyses. This work was partially supported by two PNCDI-III grants of the Romanian Ministry of Research and Innovation, PN-III-P1-1.2-PCCDI-2017-0346/29 and PN-III-P4-ID-PCCF-2016-4-0014.

REFERENCES

Andrei J., Ionescu F., 1973. *New views in the geological interpretation of the magnetic anomalies from hydrothermalized terrains from Metaliferi Mountains.* Com. IGA, IGR archive (in Romanian).

Audetat A., Pettke T., Dolejs D., 2004. *Magmatic anhydrite and calcite in the ore-forming quartz-monzodiorite magma at Santa Rita, New Mexico (USA): genetic constraints on porphyry – Cu mineralization.* Lithos, 72, 147–161.

Barth A.P., Dorais M.J., 2000. *Magmatic anhydrite in granitic rocks; First occurrence and potential petrologic consequences.* Amer. Min., 85, 430–435.

Beane R.E., Titley S.R., 1981. *Porphyry copper deposits Part II. Hydrothermal alteration and mineralization.* (Part I – Geologic settings, petrology, and tectogenesis – R.E. Titley and R.E.Beane, same vol., 214–235). Econ. Geol., 75th Anniv. Volume, 235–269.

Berbelac I., 1970. *Alunites from Voia (Metaliferi Mountains).* D.S. Inst. Geol., LVI/1, 31–50, Bucharest (In Romanian with English and French abstracts).

Berbeleac I., Zamarca A., David M., Tanasescu I., Berinde N., 1985. *The porphyry copper deposit at Voia, Metaliferi Mountains.* D.S. Inst. Geol. Geof., LXIX/2, 5–26.

Berbeleac I., 1998. *Skarns from Voia, Metaliferi Mountains, Romania.* Rom. J. Mineral. Deposits., 78, suppl., (1), 33–35.

Berbeleac I., Radulescu V., Iatan E.L., Visan M., 2012. *Relationships between crustal faults, shallow magmatic chamber and neogene porphyry Cu-Au systems at Voia, Metaliferi Mts., Romania.* Rom. J. Mineral. Deposits., 85, 1, 38–42.

Berbeleac I., Udubasa S.S., Iatan E.L., Visan M., 2014. *Geological and structural constraints on the localization of neogene porphyry-epithermal related Cu-Au (Mo), and epigenetic hydrothermal deposits/prospects from South Apusni Mts., Romania.* Rom.J.Mineral Deposits, 57, 1, 47–52.

Berbeleac I., Nutu M.-L., Chitea F., 2015. *Relationships between crustal faults, shallow magmatic chamber and neogene porphyry Cu-Au systems.* Conf. Proceed,15th Intern Multidisciplinary Sci. Geo Conf., SGEM, ISBN 978-619-7105/ISSN 1314–2704, DOI:10.5593/SGEM/2015/B11/S1.05, Book 1, vol 1, 435–442.

Blundy J., Mavrogenes J., Tattitch B., Sparks S., Gilmer A., 2015. *Generation of porphyry copper deposits by gas-brine reaction in volcanic arcs.* Nature Geosci., 8, 3, 235–240.

Bostinescu S., 1984. *Porphyry copper systems in the south Apuseni Mountains-Romania.* Ann IGG-Bucharest, LXIV, 163–174.

Burke E.A.J.,1994. *Raman microspectrometry of fluid inclusions: the daily practice.* In: DeVivo B., Frezzotti M.L.(Eds), *Fluid inclusions in Minerals: Method and Applications.* Short Course of Working group (IMA) "Inclusions in Minerals", Virginia Polythechnic Institute and State University, 25–44.

Carroll M. R., Rutherford, M. J., 1987. *The stability of igneous anhydrite: experimental results and implications for sulfur behavior in the 1982 El Chichón trachyandesite and other evolved magmas.* Journ. of Petrology 28, 781–801.

Chambefort I., Dilles J.H., Kent A.J.R., 2008. *Anhydrite-bearing andesite and dacite as a source for sulfur in magmatic-hydrothermal mineral deposits*. Geology, 36, 9, 719–722.

Dilles J.D., Kent A.J.R., Wooden J.L., Tosdal R.M., Koleszar A., Lee R.G., Farmer L.P., 2015. *Zircon compositional evidence for sulfur-degassing from ore-forming arc magmas.* Econ. Geol., 110, 241–251.

Driesner T., Heinrich, C., 2007. *The system H_2O-NaCl.Part I: Correlation formulae for phase relations in temperature-pressure-composition space from 0 to 1000°C, 0 to 5000 bar, and 0 to 1 X_{NaCl}.* Geochim. Cosmochim. Acta, 71, 4880–4901.

Ducea N.M., McInnes B.I.A., Wyllie P.J., 1999. *Experimental determination of compositional dependence of hydrous silicate melts on sulfate solubility.* Eur. J. Mineral., 11, 33–43.

Eastoe C.J., 1978. *A fluid inclusion study of the Panguna porphyry copper deposit, Bougainville, Papua New Guinea.* Econ. Geol., 73, 721–748.

Eastoe C.J., 1982. *Physics and chemistry of the hydrothermal system at the Panguna porphyry copper deposit, Bougainville, Papua New Guinea.* Econ. Geol., 77, 127–153.

Fournelle J., 1990. *Anhydrite in Nevado del Ruiz November 1985 pumice: relevance to the sulfur problem.* J. of Volc. and Geoth. Res.42, 189–201.

Fournelle J., Carmody, R., Daag, A.S., 1996. *Anhydrite-bearing pumices from the June 15, 1991, eruption of Mount Pinatubo: Geochemistry, mineralogy, and petrology.* In: Newhall, C.G., Punongbayan, R.S. (Eds.), *Fire and Mud: Eruptions and Lahars of Mount Pinatubo, Philippines.* Philippine Inst. Volcanol. Seismol., Quezon City, and Univ. Washington Press, Seattle, WA, pp. 845–863.

Frezzotti M.L., Tecce F., Casagli A., 2012. *Raman spectroscopy for fluid inclusions analysis.* Jour.of Geochem. Expl., 112, 1–20.

Fulignati P., Kamenetsky V.S., Marianelli P., Sbrana A., Mernagh T.P., 2001. *Melt inclusion record of immiscibility between silicate, hydrosaline, and carbonate melts: Applications to skarn genesis at Mount Vesuvius.* Geology, 29, 11, 1043–1046.

Gheorghita I., 1975. *Mineralogical and petrographical study of the Moldova Noua region (Suvorov-Valea Mare zone).* IGG-Bucharest, St. Th. si Ec. Ser. I, nr 11, 188p (in Romanian and English abstract).

Heinrich C.A., Driesner T., Geiger S., Landtwing M.R., 2004. *Boiling, condensation and vapor contraction: Physical fluid processes in magmatic-hydrothermal systems.* Geochim. Cosmochim. Acta, 68, S11, A295.

Henley R.W., Berger B.R., 2011. *Magmatic-vapor expansion and the formation of high-sulfidation gold deposits: chemicalk control on alteration and mineralization.* Ore Geol. Rev. 39, 63–74.

Henley R.W., King P.L., Wykes J.L., Renggli J.C., Brink F.J., Clark D.A., Troitzsch U., 2015. *Porphyry copper deposit formation by sub-volcanic sulphur dioxide flux and chemisorption.* Nature, 8, 210–215.

Jakubowski R. T., Fournelle, J., Welch, S., Swope, R. J., Camus, P., 2002. *Evidence for magmatic vapor deposition of anhydrite prior to the 1991 climactic eruption of Mount Pinatubo, Philippines.* Amer. Min. 87, 1029–1045.

John D.A., Ayuso R.A., Barton M.D., Blakely R.J., Bodnar R.J., Dilles J.H., Gray Floyd Graybeal F.T., Mars J.C., McPhee D.K., Seal R.R., Taylor R.D., Vikre P.G., 2010. *Porphyry copper deposit model*, Chap. B of *Mineral deposit models for resource assessment*: U.S. Geological Survey Scientific Investigations Report 2010–5070–B, 169 p.

Kotelnikova Z.A., Kotelnikov A.R., 2010. *Immiscibility in sulfate-bearing fluid system at high temperatures and pressures.* Geochem. Internat., 48, 4, 381–389.

Li C., Ripley E.M., Naldrett A.J., Schmitt A.K., Moore C.H., 2009. *Magmatic anhydrite-sulfide assemblages in the plumbing system of the Siberian Traps.* Geology, 37, 3, 259–262.

Luhr J. F., Carmichael I. S. E., Varekamp, J. C., 1984. *The 1982 eruptions of El Chichon volcano, Chiapas, Mexico: mineralogy and petrology of the anhydrite-bearing pumices.* Journal of Volcanology and Geothermal Research 23, 69–108.

Meinhold G., 2010. *Rutile and its applications in earth sciences.* Eart-Sci. Rev., 102, 1–28.

Milu V., Milesi J.P., Leroy, J.L., 2004. *Rosia Poieni copper deposit, Apuseni Mountains, Romania: Advanced argillic overprint of a porphyry system*. Mineralium Deposita, v. 39, 173−188.

Newton R. C., Manning C. E., 2002. *Experimental determination of calcite solubility in H_2O-NaCl solutions at deep crust/upper mantle pressures and temperatures: implications for metasomatic processes in shear zones.* Amer. Min., 87, 1401–1409.

Newton R.C., Manning C.E., 2005. *Solubility of anhydrite, $CaSO_4$, in NaCl-H_2O solutions at high pressures and temperatures: applications to fluid – rock interaction.* Journ. of Petrology, 46, 4, 701–706.

Pasteris J. D., Wopenka B., Wang, A., Harris, T. N.,1996. *Relative timing of fluid and anhydrite saturation: another consideration in the sulfur budget of the Mount Pinatubo eruption.* In: Newhall, F. G. & Punongbayan, R. S. (eds) Fire and Mud. Seattle: University of Washington Press, pp. 875–891.

Parat F., Dungan M. A., Streck, M. J., 2002. *Anhydrite, pyrrhotite, and sulfur-rich apatite: tracing the sulfur evolution of an Oligocene andesite (Eagle Mountain, CO, USA).* Lithos, 64, 63–75.

Penniston-Dorland S.C., 2001. *Illumination of vein quartz textures in a porphyry copper ore deposit using scanned cathodoluminescence: Grasberg Igneous Complex, Irian Jaya, Indonesia.* Amer. Min., 86, 652–666.

Pintea I., 1993a. *Microthermometry of the hydrosaline melt inclusions from copper – porphyry ore deposits (Apuseni Mountains, Romania).* Arch. Mineral. XLIX,165–167, Warsaw, Poland.

Pintea I., 1993b. *Fluid inclusion studies in anhydrite crystals of some tertiary porphyry-copper systems from Apuseni Mountains (Romania).* The 2th Edition of the National Miner. Symp., July 5–11, oral presentation. Timisoara, Romania.

Pintea I., 1996. *Fluid inclusions study with special view on fluid phases immiscibility associated to porphyry copper genesis from Metaliferi Mountains.* Ph D thesis, Univ Bucharest (in Romanian). 172p.

Pintea I., 2009. *Still problematic facts on the fate of brines in the alpine porphyry copper systems in Romania.* ECROFI XX, Granada (Spania) abstr. 187–188.

Pintea I., 2010. *Fluid and melt inclusions evidences for autometasomatism and remelting in the alpine porphyry copper genesis from Romania.* Rom. J. Mineral Deposits., 84 Spec. issue, 15–18. The 7th Nat Symp on Econ. Geol., "Mineral Resources of Carpathians area", 10–12 Sept., 2010, Baia Mare.

Pintea I., 2014a. *The magmatic immiscibility between silicate-, brine-, and Fe-S-O melts from the porphyry (Cu-Au-Mo) deposits in the Carpathians (Romania): a review.* Romanian Journal of Earth Sci. 87, 1, 32p, first on line at www.igr.ro.

Pintea I., 2014b. *Magmatic and hydrothermal features of the fluid and melt inclusions from the quartz xenoliths, fragments and phenocrysts from Săpânţa Valley (Igniş Mountains, Romania).* Rom. J. Mineral. Deposits. 87, 1, 79–82.

Pintea I., 2016. *A self-perspective research topic revealed during the elaboration of the atlas "Fluid and Melt Inclusions from Romania".* Rom. J. Mineral. Deposits, 89, 1–2, 1–6.

Rabbia O.M., Hernandez L.R., French D.H., King R.W., Ayers J.C., 2009. *The El Teniente porphyry Cu-Mo deposit from a hydrothermal rutile perspective.* Miner Deposita, 44, 8, 849–866.

Rusk B., and Reed, M., 2002. *Scanning electron microscope-cathodoluminescence analysis of quartz reveals complex growth histories in veins from the Butte porphyry copper deposit, Montana.* Geology, v. 30, p. 727–730.

Seedorff E., Dilles J.H., Proffett J.M. Jr., Einaudi M.T., Zurcher L., Stavast W.J.A., Johnson D.A., Barton M.D., 2005. *Porphyry deposits: characteristics and origin of hypogene features.* Econ. Geol., 100th Anniv. Vol., 251–298.

Stefanescu M., 1986, *Profiles elaboration, scale 1:200 000, for completing the geological image of Romania.* Geological Institute of Romania, Bucharest (in Romanian).

Stern C.R., Funk J.A., Skewes A.M., 2007. *Magmatic anhydrite in plutonic rocks at the El Teniente Cu-Mo deposit, Chile, and the role of sulfur- and copper-rich magmas in its formation.* Econ. Geol., 102, 1335–1344.

Streck M. J., Dilles, J. H., 1998. *Sulfur evolution of oxidized arc magmas as recorded in apatite from a porphyry copper batholith.* Geology 26, 523–526.

Student J.J. Bodnar R.J., 2004. *Silicate melt inclusions in porphyry copper deposits: Identification and homogenization behavior.* Canadian Mineral. 42, 1583–1599.

Udubaşa G., Rosu E., Seghedi I., Ivascanu P.M.,2001. *The "Golden Quadrangle" in the Metaliferi Mts. Romania: what does this realy mean?* Rom. J. Mineral Deposits, vol. 79 suppl. 2, Abstract volume, ABCD-GEODE 2001 workshop Vata Bai, Romania, 24–34.

Vasyukova O.V., 2011. *Types and origin of quartz and quartz-hosted fluid inclusions in mineralised porphyries.* Ph.D. thesis, University of Tasmania, Hobart, 213 p.

Wilkinson J.J., Vasyukova O., Laird J.S., Ryan C., Kamenetsky D., 2015. *Hydrosilicate liquids: unconventional agents of metal transport in porphyry ore systems.* ECROFI –XXIII, Leeds-UK, 27–29 June, 2015, Extended abstract Vol., p. 116.

Williams S.A., Cesbron F.P., 1977. *Rutile and apatite: useful prospecting guides for porphyry copper deposits.* Min. Mag., 41, 288–292.